

# Searching for Alternatively Spliced Variants of Phospholipase Domain-Containing 2 (*Pnpla2*), a Novel Gene in the Retina

Jacqueline Talea DesJardin, S Patricia Becerra and Preeti Subramanian\*

Section of Protein Structure and Function, Laboratory of Retinal Cell and Molecular Biology, National Eye Institute, National Institutes of Health, Bethesda, MD 20892-0608, USA

## Abstract

**Purpose:** Ensembl and other expressed sequence tag (EST) databases reveal putative alternative splice variants in mouse and rat for *Pnpla2*, the gene encoding pigment epithelium-derived factor-receptor (PEDF-R). The purpose of this study was to obtain experimental evidence for *Pnpla2* splice variants in mouse.

**Materials and Methods:** Cultures of a mouse cell line derived from photoreceptors (661W cells) and mouse eye, heart, adipose, kidney, and liver tissues were used. Messenger RNA (mRNA) was isolated from cells and tissues, and complementary DNA (cDNA) was synthesized. Polymerase chain reaction (PCR) primer pairs were designed to flank the putative splice sites. Exon exclusion real time PCR was used to reduce amplification of the full-length *Pnpla2* transcript and enhance amplification of low abundant splice variants. PCR products were resolved by agarose gel electrophoresis and detected with a UV transilluminator. Recombinant plasmids containing a human full-length *PNPLA2* cDNA or a *PNPLA2* cDNA lacking exon 5b (E5b) were controls to validate the techniques. Total cell lysates from 661W cells were prepared. PEDF-R protein detection was performed using western blots.

**Results:** PCR products for *Pnpla2* transcripts obtained from 661W cells or various mouse tissues resolved into a single band following amplification with multiple primer pairs. Simultaneous amplification of two *PNPLA2* cDNAs at various molar ratios prevented the detection of lower abundant transcripts. However, even when the cDNA for the full-length *Pnpla2* transcript was significantly excluded using the exon exclusion method, no bands corresponding to *Pnpla2* splice variants were detectable. Nonetheless, western blots of total 661W cell lysates with two different antibodies revealed isoforms for the PEDF-R protein.

**Conclusions:** The data provide evidence for the existence of a single, full-length *Pnpla2* transcript that could give rise to a single protein product that undergoes posttranslational processing.

**Keywords:** *Pnpla2*; Alternative splicing; PEDF; PEDF-R; Retina

## Introduction

In recent years, a group of genes encoding proteins with a common domain termed patatin-like phospholipase (PNPLA domain) has been discovered in the human genome. There are nine members of the PNPLA family, all of which display lipase, phospholipase and transacylase enzymatic activities and have major roles in adipocyte differentiation, lipid metabolism and signaling [1,2]. One PNPLA gene, *PNPLA2* codes for a protein that is present at high levels in adipose tissue as a triglyceride lipase involved in lipid turnover [3]. Interestingly, we have reported that the retina expresses *PNPLA2* and its gene product PEDF-R throughout the retinal pigment epithelium, photoreceptors, and the ganglion cell layer [4-7]. PEDF-R acts as a cell-surface receptor for pigment epithelium-derived factor (PEDF) [8], a key factor for the neural and vascular retina [9-11]. It exhibits phospholipase activity that hydrolyzes the sn-2 acyl bond of phospholipid substrates to release lysophospholipid and fatty acids [4,5,8]. PEDF binding stimulates the PLA<sub>2</sub> activity of PEDF-R [4,5,8], and in turn its fatty acid products can act as bioactive lipid second messengers to trigger downstream antiapoptotic signaling in retina cells [12]. The PEDF-R polypeptide sequence has a patatin-like phospholipase domain towards its amino end (10-179) and amino acids serine in position 47 (Ser<sup>47</sup>) and aspartic acid in position 166 (Asp<sup>166</sup>) form the catalytic dyad of the enzymatic active site [6-8]. Recently, we have mapped a functional PEDF binding region in PEDF-R (Threonine 210 (Thr210) to Leucine 232 (Leu232)) located on exon 5b of human *PNPLA2* (Figure 5A) [8]. Moreover, the *PNPLA2* gene plays a crucial role in human embryonic stem cell self-renewal [13], human melanoma metastasis inhibition [14], and human prostate cell growth inhibition [15], all of which depend on PEDF.

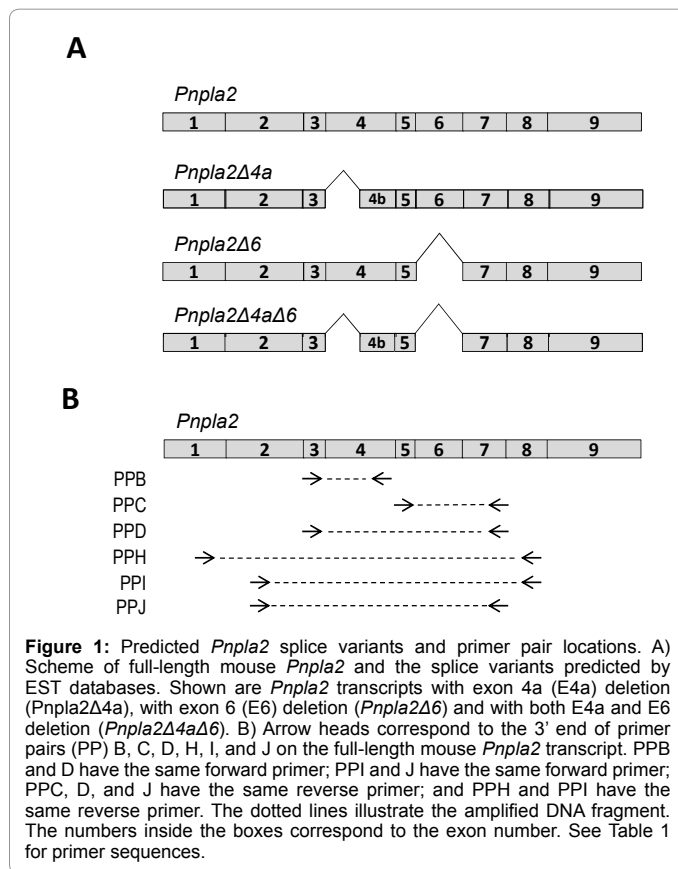
Alternative splicing is a common posttranscriptional process for protein diversification, with the majority of the human genes potentially giving rise to multiple variants and thus creating protein isoforms [16]. The human *PNPLA2* gene has ten exons of which exons 2-10 are the coding exons and the mouse *Pnpla2* gene contains nine exons, with a coding capacity of 504 and 486 amino acids, respectively. The *PNPLA2* sequence is highly conserved among the mammalian species, with mouse and human species having 87% identity. Alternatively spliced *Pnpla2* variants are predicted in mouse: one with partial E4 exon deletion (E4a) (*Pnpla2Δ4a*; base pairs 487 - 589), another with an exon 6 (E6) deletion (*Pnpla2Δ6*; base pairs 758 - 925) and a third with both the E4a and E6 deletions in the same transcript (*Pnpla2Δ4aΔ6*) (Figure 1A). The first alternative splice transcript would generate a protein without Asp<sup>166</sup> of the catalytic dyad, implying an inactive PEDF-R that could have implications in disease progression where PEDF-R is unable to mediate the effects of PEDF. The second one encodes part of

\*Corresponding author: Preeti Subramanian, NEI-NIH, Bldg. 6, Rm. 131F, 6 Center Dr., MSC 0608, Bethesda, MD 20892-0608, USA, Tel: 301-451-1970; Fax: 301-402-1883; E-mail: [subramanianp@nei.nih.gov](mailto:subramanianp@nei.nih.gov)

Received July 02, 2013; Accepted September 02, 2013; Published September 09, 2013

**Citation:** DesJardin JT, Becerra SP, Subramanian P (2013) Searching for Alternatively Spliced Variants of Phospholipase Domain-Containing 2 (*Pnpla2*), a Novel Gene in the Retina. J Clin Exp Ophthalmol 4: 295. doi:10.4172/2155-9570.1000295

**Copyright:** © 2013 DesJardin JT, et al. This is an open-access article distributed under the terms of the Creative Commons Attribution License, which permits unrestricted use, distribution, and reproduction in any medium, provided the original author and source are credited.



the extracellular domain of PEDF-R; however, it is unclear what the functional importance of E6 is to PEDF-R activity. While the E6 region of mice (E7 of human) is not necessary for the binding of PEDF, the possibility that this region plays an indirect role in interactions with PEDF remain to be explored.

Although databases predict alternative splicing for the *Pnpla2* mRNA in mouse, it is not yet known whether multiple variants exist. It is of interest to obtain empirical evidence for alternative splice variants to understand the regulation of PEDF-R, which would have an impact on PEDF activity. In this study, we used RT-PCR-based methods to explore the predicted alternative splicing of *Pnpla2*. For this purpose, we used 661W cells, a mouse cone photoreceptor cell line that has been shown to respond to PEDF treatment in the event of light damage [17] and also mouse eye, heart, adipose, liver, and kidney tissues. With the tested samples, one main *Pnpla2* transcript was detected.

## Materials and Method

### Cell culture

Photoreceptor-derived 661W cells (kind gift from Dr. Muayyad Al-Ubaidi, University of Oklahoma Health Sciences) were cultured in DMEM medium with 10% of fetal bovine serum (FBS) at 37°C with 5% CO<sub>2</sub> and 95% humidity.

### Expression vector/plasmid

Two *PNPLA2*-containing expression vectors were used: PEDF-R, containing the full-length human *PNPLA2* open reading frame (ORF) of 1512 bp and PEDF-RΔE5b, containing a human *PNPLA2* cDNA missing the 90 base pairs of exon 5b (E5b; bp 607-696). *PNPLA2* cDNA

for PEDF-R and PEDF-RΔE5b were constructed into pEXP1-DEST vectors with N-terminal epitope-tags (N-end-His6/Xpress) under a T7 transcription promoter as previously described [4].

### RNA extraction, cDNA synthesis and real-time PCR

For 661W cells, total RNA was purified using the RNeasy™ mini kit (Qiagen) according to the manufacturer's instructions. For tissue samples (kind gift from Dr. Lars Von Buchholtz, NIDCR, National Institutes of Health), total RNA was isolated from fresh mouse tissues using TRIzol (Invitrogen) according to the manufacturer's instructions. RNA concentrations were determined using the Beckman DU 640 Spectrophotometer. The mRNA (1-5 μg) was reverse-transcribed using SuperScript III First-Strand Synthesis System (Invitrogen) in a total volume of 20 μL.

*Pnpla2* transcript was amplified in a total volume of 25 μL containing 400 nM forward primer, 400 nM reverse primer, 2X SYBR Green mix (Qiagen), and 2 μL cDNA in the Bio-Rad Chromo4 real-time system. All primers (Table 1) were custom synthesized by Invitrogen. The thermal cycling conditions were 95°C for 15 min, then 46 cycles of 95°C for 30 s to 1 min, 60°C for 30 s to 1 min, and 72°C for 30 s to 1 min.

### Exon exclusion

The restriction endonucleases *AclI* (New England BioLabs, R0641S), *MfeI* (New England BioLabs, R0589S), and *BstEII* (New England BioLabs, R0162S) were used. Deoxyoligonucleotides (custom synthesized by Invitrogen) were designed with sequences complementary to regions within E4a (5'-**TGAGCTGAAGAAT ACCATCACAGTGTCCCCAT**Ccc-3'), E6 (5'-CTGGAGAGGAGGATCAATTGCAGCCTTA TAGAcc-3'), or E5b (5'-CACGAGCTGCGGGTACCAACACCAGCATCCAcc-3'), included the cleavage recognition sites (shown in bold) and, to prevent PCR amplification, contained two unpaired nucleotides at the 3' end (shown in lower case). As in Wang et al. [18], the deoxyoligonucleotides (1 μM) were annealed by mixing with cDNA in a total volume of 20 μL and heating at 94°C for 2 min, 85°C for 15 min, 70°C for 15 min, 55°C for 15 min and 25°C for 15 min. Restriction enzymes (12.5 - 25 units) or equal volume of water (for "buffer" controls) were added with the provided digestion buffer and incubated at 37°C for 1 hour. *CutSmart™* buffer (50 mM potassium acetate, 20 mM Tris-acetate, 10 mM magnesium acetate, 100 μg/mL BSA, pH 7.9) was used for restriction digestion reactions. Following the restriction digest 2 μL of the product was used for RT-PCR amplification. While *Pnpla2* has only one cleavage recognition site for *MfeI*, it has two for each *BstEII* and *AclI*. Amplification primer pairs (PPI or J) were chosen such that the additional site was excluded. Both primer pairs had the same forward primer (Figure 1B).

### Agarose gel electrophoresis

PCR products were diluted 1:5 or 1:10 and a total of 20 μL was loaded into either 1.2% or 2% agarose E-gels (Invitrogen). The gels, containing ethidium bromide, were run for 30-45 minutes using the E-Gel PowerBase™ v.4 (Invitrogen). Photographs were taken with a UV transilluminator. The TrackIt™ 100 bp DNA ladder (Invitrogen) or the 1Kb Plus DNA ladder (Invitrogen) was used to estimate molecular weights of DNA fragments.

### Recombinant protein, cell lysate preparation and western blotting

Total cell lysate from 661W cells was prepared with RIPA buffer

Primer Pair Name	Primer Sequences <sup>a</sup>	Template <sup>b</sup>	Expected PCR Product Size (bp) <sup>c</sup>
PPB	5'-tgtggcctcattctctctac-3'	<i>PNPLA2</i>	217
	5'-tcgagaggcggtagagattg-3'	<i>PNPLA2Δ4a</i>	115
PPC	5'-tccgagagatgtgcaaacag-3'	<i>PNPLA2</i>	361
	5'-aacggatggtgaaggacac-3'	<i>PNPLA2Δ6</i>	193
PPD	5'-tgtggcctcattctctctac-3'	<i>PNPLA2</i>	608
		<i>PNPLA2Δ4a</i>	506
	5'-aacggatggtgaaggacac-3'	<i>PNPLA2Δ6</i>	440
		<i>PNPLA2Δ4aΔ6</i>	338
PPH	5'-aacgccactcacatctacg-3'	<i>PNPLA2</i>	1025
		<i>PNPLA2Δ4a</i>	923
	5'-accagatctggcagatgct-3'	<i>PNPLA2Δ6</i>	857
		<i>PNPLA2Δ4aΔ6</i>	755
PPI	5'-atccctctcaacctggt-3'	PEDF-R	1019
		PEDF-RΔE5b	929
		<i>PNPLA2</i>	886
		<i>PNPLA2 Δ4a</i>	784
	5'-accagatctggcagatgct-3'	<i>PNPLA2 Δ6</i>	718
		<i>PNPLA2 Δ4aΔ6</i>	616
PPJ	5'-atccctctcaacctggt-3'	PEDF-R	880
		PEDF-RΔE5b	790
		<i>PNPLA2</i>	808
	5'-aacggatggtgaaggacac-3'	<i>PNPLA2 Δ4a</i>	706
		<i>PNPLA2 Δ6</i>	640
		<i>PNPLA2 Δ4aΔ6</i>	538

<sup>a</sup>Sequence of forward (top) and reverse (bottom) primers for each primer pair. (Note, PPB and D have the same forward primer, PPC and D have the same reverse primer, and PPH and PPI have the same reverse primer) Bolded and underlined letters indicate base pairs, which deviate in the human *PNPLA2* sequence in PPH and I.  
<sup>b</sup>Potential *Pnpla2/PNPLA2* transcripts expected to be amplified by each primer pair. *Pnpla2*, full-length mouse *Pnpla2* transcript. *Pnpla2Δ4a*, mouse cDNA of a *Pnpla2* splice variant without exon 4a (E4a). *Pnpla2Δ6*, mouse cDNA of a *Pnpla2* splice variant without exon 6 (E6). *Pnpla2Δ4aΔ6*, mouse cDNA of a *Pnpla2* splice variant without E4a or E6. PEDF-R, expression vector containing full-length human *PNPLA2* cDNA. PEDFRΔE5b, expression plasmid containing human *PNPLA2* cDNA lacking exon 5b.  
<sup>c</sup>Expected PCR product sizes, in base pairs, resulting from amplification with the indicated primer pair and the indicated *Pnpla2/PNPLA2* transcript.

**Table 1:** Primer pairs used for PCR amplification of *Pnpla2/PNPLA2* transcripts.

(Thermo Scientific). Protein concentration was determined with BCA Protein Assay (Pierce). Expression of PEDF-R was performed using the pEXP1-PEDF-R vector and cell-free *in vitro* protein synthesis using *E. coli* extracts from IVPS<sup>TM</sup> (Invitrogen). The particulate material was separated from the soluble by centrifugation (14,000 X g, 4°C, 5 min) and the pellet was resuspended in SDS-PAGE sample buffer.

### Polyacrylamide Gel Electrophoresis

Protein samples were applied to NuPAGE 4-12% polyacrylamide gels in Bis-Tris buffer with NuPAGE MOPS SDS as running buffer (Invitrogen). After electrophoresis, proteins from the gel were transferred to nitrocellulose membranes using the iBlot Gel Transfer system (Invitrogen) for immuno-blot. Prestained ladders (Bio-Rad, Cat#161-0305) were used for molecular weight markers.

### Immuno-Blot

Total protein detection in nitrocellulose membranes was accomplished with Ponceau Red. Nitrocellulose membranes were incubated in blocking solution for 1 hour at room temperature and then in blocking solution with one of the following PEDF-R antibodies: SAB2500132 (Sigma) or AF5365 (R&D Systems) overnight at 4°C. For SAB2500132, 3% milk in TBS-T was used for blocking and primary antibody dilutions and 5% milk in TBS-T was used for secondary dilutions; for AF5365, the blocking solution was 1% BSA in TBS-T. Each anti-PEDF-R antibody was diluted in blocking solution in 1:250 (SAB2500132) or 1:500 (AF5365) dilutions, followed by HRP-conjugated rabbit anti-goat (1:25,000, Sigma) or donkey anti-sheep IgG

(1:20,000, Sigma), respectively. For anti-Xpress antibody (Invitrogen, cat#R910-25), primary dilution was 1:10,000 in 1% BSA in TBS-T and secondary dilution was 1:200,000 of HRP-conjugated goat anti-mouse. Chemiluminescence detection was performed with Super Signal West Dura Extended Duration Substrate (Thermo Scientific) on X-Ray films.

## Results

### Potential alternative splice transcripts for *Pnpla2*

Databases such as the Ensembl (<http://useast.ensembl.org/index.html>) and the UCSC genome browser (<http://genome.ucsc.edu/>) reveal two potential alternatively spliced *Pnpla2* transcripts in the mouse genome [19,20]. These predictions are based on expressed sequence tags (ESTs), which are short (200-800 base pairs) single-pass sequence reads that contains partial coverage and thereby possible sequence errors [21]. For the mouse sequence, one potential transcript has an E4a deletion (*Pnpla2Δ4a*; bp 487 - 589), the other has an E6 deletion (*Pnpla2Δ6*; bp 758 - 925) and a third has both E4a and E6 deletion (*Pnpla2Δ4aΔ6*). Figure 1A shows a scheme of the predicted *Pnpla2* mRNAs (*Pnpla2Δ4a*, *Pnpla2Δ6* and *Pnpla2Δ4aΔ6*). The above observations led us to explore if the potential alternative splice transcripts for mouse *Pnpla2* exist *in vivo*.

### *Pnpla2* transcript from 661W cells

To empirically determine the expression of *Pnpla2* transcripts in mouse, we performed RT-PCR using cDNAs from mRNA of 661W cells. Figure 1B shows primer pairs designed to amplify *Pnpla2* cDNAs by RT-PCR. Primer pairs (PP) B, C, and D were used to detect full-

length *Pnpla2* as well as the putative spliced *Pnpla2Δ4a*, *PNPLA2Δ6*, and *Pnpla2Δ4aΔ6* transcripts. PPD has the same forward primer as PPB and the same reverse primer as PPC. Amplification of cDNA fragments was expected to result in discrete and distinct lengths for each primer pair (Table 1). Figure 2 shows PCR products with the three primer pairs and 661W cDNA separated by gel electrophoresis, and reveals that each primer pair amplified a single band that migrated as a DNA fragment of the expected size for *Pnpla2*. Our data show a single, full-length *Pnpla2* transcript in 661W cells.

### *Pnpla2* transcript from mouse tissues

The UCSC genome browser suggests that *Pnpla2* splice variants were detected in ESTs obtained from mouse mammary tumor (*Pnpla2Δ4a*) or mouse kidney (*Pnpla2Δ6*), and so we hypothesized that the expression of splice variants may be tissue-dependent [20].

To test this hypothesis, we employed the same method as above, using cDNA from mouse eye, heart, adipose, kidney, and liver tissues for amplification. Amplification with PPB, C, or D in mouse tissues was anticipated to result in the same sized PCR products as was expected for the 661W cells (Table 1). We found that amplification using any of the three primer pairs in any of the five tissues yielded a distinct single band of PCR product that migrated as DNA of the size expected for *Pnpla2* (Figure 3). Again, our data show that a single *Pnpla2* transcript was detected in mouse tissues as in 661W cells.

### Limitations of low abundant transcript detection

As previously described, low abundant alternatively spliced transcripts may not be amplified at the same rate as a more abundant transcript, and would therefore be undetectable [18]. To determine if these limitations apply to our study, we designed an experiment in which cDNAs with deletions to emulate spliced regions were used at various ratios as templates in PCR reactions. Expression plasmids containing the full-length human *PNPLA* cDNA (PEDF-R) and a deletion of 90 base pairs of the 3' end region of human exon 5 (mouse exon 4) (PEDF-RΔE5b) were used as templates to validate our assay (Figure 4A). Two new primer pairs were designed (PPH and I) to be as homologous as possible to mouse and human sequences of *Pnpla2/PNPLA2*. The primer pairs have different forward primers and share

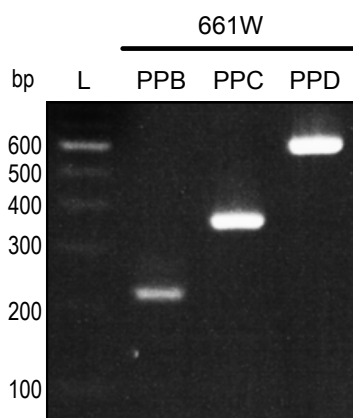


**Figure 2:** RT-PCR of *Pnpla2* transcript from 661W cells. Amplification of *Pnpla2* cDNA from 661W cells using PPB, C, or D was performed as in methods. PCR products were diluted 1:10 and resolved by 2% agarose E-gel electrophoresis. DNA was stained with ethidium bromide. Photograph of the UV exposed gels is shown. Numbers on left indicate migration pattern of DNA ladder (L). Primer pairs used for each PCR product are indicated at the top. See Table 1 for expected product sizes.

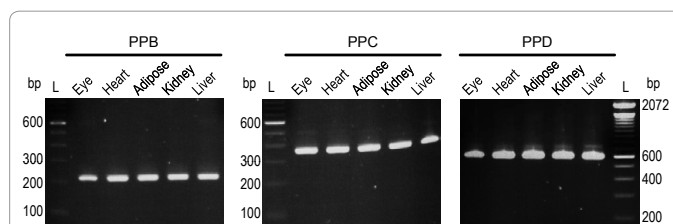


**Figure 3:** RT-PCR of *Pnpla2* transcript from mouse tissues. Amplification of *Pnpla2* cDNA from mouse eye, heart, adipose, kidney, and liver tissues using primer pair (PP) B, C, or D and analyzed as in Figure 2. Numbers indicate migration pattern of DNA ladder (L). See Table 1 for expected product sizes.

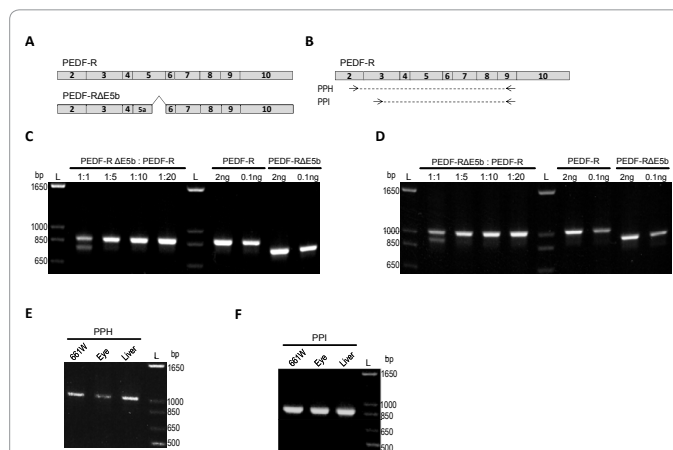


**Figure 4:** Detection limits of low abundant transcripts. A) Schematic of the open reading frame of full-length human *PNPLA2* cDNA (PEDF-R) or a *PNPLA2* cDNA lacking E5b (PEDF-RΔE5B) expression plasmid. B) Location of primer pairs (PP) H and I on the full-length human *Pnpla2* transcript. The location for the primer pairs on the mouse *Pnpla2* transcript are in Figure 1B, 1C and 1D) The plasmids were mixed in 1:1 (5ng each), 1:5 (2ng PEDF-RΔE5b, 8 ng PEDF-R), 1:10 (1 ng PEDF-RΔE5b, 9 ng PEDF-R), or 1:20 (0.5 ng PEDF-RΔE5b, 9.5 ng PEDF-R) molar ratios prior to PCR amplification with PPH (C) or PPI (D). Also shown is amplification with specified amounts (0.1 or 2 ng) of each plasmid alone with PPH or PPI. E, F) Amplification of *Pnpla2* transcripts from 661W cells as well as mouse eye and liver tissues was tested with both PPH (E) and PPI (F). For C-E, PCR products were diluted 1:10, resolved by 1.2% agarose E-gel electrophoresis, and stained with ethidium bromide. Photographs of UV exposed gels are shown. Numbers indicate migration pattern of DNA ladder. See Table 1 for expected product sizes.

the same reverse primer (Figure 4B). The sequences of the two forward primers and the reverse primer were identical to the mouse *Pnpla2* sequence, but each primer diverged by a single base pair from the human *PNPLA2* sequence. Nonetheless, both PPH and PPI amplified mouse and human *Pnpla2/PNPLA2* transcripts from expression plasmids. Plasmids PEDFRΔE5b and PEDF-R were mixed in various molar ratios: 1:1 (5 ng to 5 ng), 1:5 (2 ng to 8 ng), 1:10 (1 ng to 9 ng), or 1:20 (0.5 ng to 9.5 ng) prior to PCR amplification. Products were detected with *PNPLA2* and *PNPLA2ΔE5b* at the 1:1 molar ratio with both PPH (Figure 4C) and PPI (Figure 4D). However, at ratios 1:5 and lower of PEDF-RΔE5b to PEDF-R, PEDFRΔE5b could not be detected when amplified with either primer pair. We noted that when a low amount (e.g. 0.1 ng) of either plasmid was used as the PCR template by itself, amplification with either PPH (Figure 4C) or PPI (Figure 4D) could be easily detected. These results indicate that amplification of the low abundant PEDFRΔE5b was inhibited by competition with the more highly abundant PEDF-R.

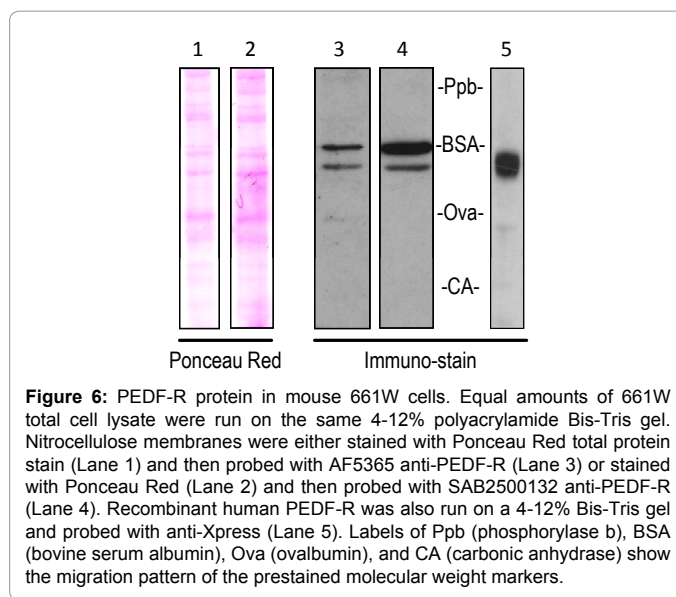
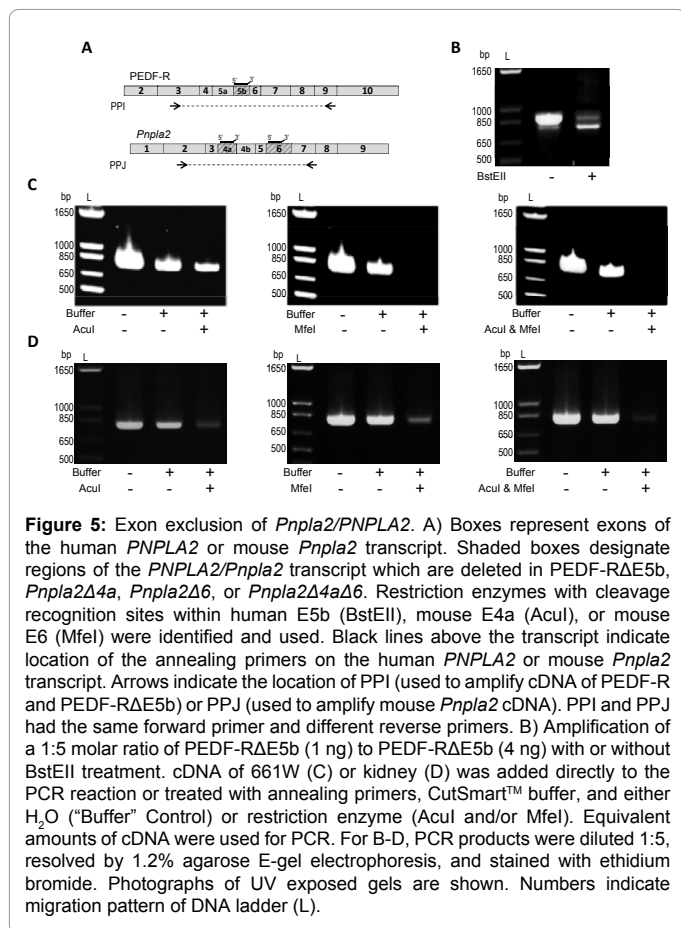
We also used PPH and PPI to test a subset of mouse cDNA samples

(661W cells, eye tissue, and liver tissue) to detect *Pnpla2* transcript. In all three samples of cDNA, with either PPH or PPI, a single DNA of the size expected for *Pnpla2* (Table 1) was detected (Figure 4E-4F), implying a single transcript.

### Exon exclusion for cleavage of full-length *Pnpla2*/PNPLA2 transcript

To reduce competition between the multiple *Pnpla2*/PNPLA2 transcripts, we used the exon excision method in which cDNA amplification of the highly abundant transcript is limited by endonuclease digestion at a chosen exon. It was expected that introduction of the restriction digestion step would significantly reduce competition and allow amplification of the low abundant transcripts that do not have the chosen exon [18]. We identified that the human E5b region of PNPLA2 has a BstEII restriction recognition site (Figure 5A), which is missing in PEDF-RΔE5b plasmid. When a 1:5 molar ratio of PEDF-RΔE5b to PEDF-R (4 ng to 1 ng) was amplified and resolved by gel electrophoresis, the PCR reaction yielded products of ~880 bp (size expected for PNPLA2) and ~790 bp (size expected for PNPLA2ΔE5b), with the top band appearing significantly more intense than the bottom band (Figure 5B). However, Figure 5B also shows that when the 1:5 molar ratio was treated with BstEII prior to amplification, the bottom band increased in intensity and the top band decreased in intensity. These findings indicate that we successfully decreased PNPLA2 amplification to allow for greater detection of the low abundant PNPLA2ΔE5b transcript.

Exon region E4a and E6 have cleavage recognition sites for *AcuI*



and *MfeI* enzymes, respectively. When using the *AcuI* and/or *MfeI* restriction enzymes on 661W or mouse kidney cDNA, we found similar efficiency in reducing the amplification of the full-length *Pnpla2* transcript. Controls with cDNA under the same condition as above in the absence of restriction enzyme ("Buffer" control) yielded a single band as expected for the high abundance full-length *Pnpla2*. We found that treatment with *AcuI* and/or *MfeI* reduced the intensity of the ~808 bp product (size expected for full-length *Pnpla2*) for 661W (Figure 5c) and for kidney cDNA (Figure 5D). Despite this, no additional band corresponding to DNA fragments of the size expected for *Pnpla2*Δ4a, *Pnpla2*Δ6, or *Pnpla2*Δ4aΔ6 was detected (Figures 5C and 5D), even when loading greater amounts of PCR product (data not shown). Thus, our data point to the presence of a single *Pnpla2* transcript in mouse cells and tissues, even after significantly improving the sensitivity of our method for low abundant transcripts by excluding the cDNA of the large transcript.

### PEDF-R protein in mouse 661W cells

To analyze the protein product of the mouse *Pnpla2* transcript, we performed western blots of 661W total cell lysate with two anti-PEDF-R antibodies (AF5365 or SAB2500132) recognizing different epitopes. AF5363 recognizes a 92 amino acid PEDF-R segment encoded by exons 4 and 5 of mouse *Pnpla2*. SAB2500132 recognizes a 12 amino acid PEDF-R segment encoded by exon 2 of human PNPLA2. Blots probed with either antibody in 661W total cell lysate yielded at least two protein bands, with the slower migrating one being more intense (Figure 6). Additional bands were detected at longer exposure of the x-ray film, suggesting other possible PEDF-R isoforms (data not shown). The migration position of mouse PEDF-R was compared to the recombinant human N-end-His<sub>6</sub>/Xpress PEDF-R, which has 553 amino acids. Figure 6 shows that the more intense bands in lanes 3 and 4 correspond to proteins with apparent molecular weights that are higher than that of the recombinant protein.

### Discussion

In this study, alternative splicing was examined in biological samples because mouse *Pnpla2* has two potential alternatively spliced transcripts *in silico*. Despite the prediction of alternatively spliced PNPLA2 transcripts, we detected only a single *Pnpla2* transcript in

661W cells and mouse eye, heart, adipose, liver, and kidney tissues. This could be due to one of three reasons: 1) only one *Pnpla2* transcript exists, 2) the levels of alternatively spliced transcripts are too low to be detected by these methods, or 3) the alternative splicing of *Pnpla2* mRNAs might be tissue specific or regulated by disease progression.

RT-PCR is the most commonly employed technique for validating alternative splicing. Generally, as in this study, simultaneous amplification of cDNA of variant transcripts occurs with primer pairs designed to flank potential splice sites. The limitations of simultaneous detection of high and low abundant transcripts pose a problem. This was clearly demonstrated with cDNAs containing PEDF-R and PEDF-RΔE5b in various molar ratios. Our data are in agreement with reports that competition between cDNAs of variant transcripts results in inhibition of the amplification of the cDNA for the less abundant transcript [18]. One approach to overcome this limitation can be achieved using an exon exclusion approach. The use of restriction enzymes to specifically cleave human E5b, mouse E4a, and/or mouse E6 allows for more sensitive detection of less abundant transcripts, as evident in our experiments with PEDF-RΔE5b cDNAs (Figure 5B). Despite significantly reducing the intensity of the band corresponding to full-length *Pnpla2* in 661W and mouse kidney cDNA, we still detected a single band corresponding to *Pnpla2* with no other transcript (Figure 5B-5D). Therefore, the presence of the low abundant *Pnpla2Δ4a*, *Pnpla2Δ6*, and *Pnpla2Δ4aΔ6* splice variants seems unlikely. Furthermore, if they do exist, these transcripts would be in such low abundance that their role in any significant biological activity would be questionable.

Alternative splicing is commonly regulated by a number of developmental, environmental, and cell specific factors. It is likely that the cells and tissues selected in these experiments do not express the alternatively spliced transcripts. Interestingly, EST databases indicate that the *Pnpla2Δ4a* transcript is detected in mouse mammary tumor tissue, suggesting this transcript may be cancer-specific or up-regulated in certain disease states. However, it remains to be determined if mouse cancer cells contain an extra transcript for *Pnpla2*. On the other hand, the EST databases specify that the *Pnpla2Δ6* transcript is identified in adult mouse kidney tissue. Even with the highly sensitive exon exclusion technique, we could not detect *Pnpla2Δ6* in our kidney samples.

Our data point to the existence of a single *Pnpla2* transcript in the mouse 661W cell line and mouse eye, heart, adipose, liver, and kidney tissues. Detection of two PEDF-R protein bands in 661W cells suggests posttranslational processing might occur. The lower molecular weight protein observed here seems to be consistent with the size of the mouse PEDF-R protein precursor. Thus, the single transcript can give rise to a single protein product that may undergo posttranslational modifications, resulting in the larger PEDF-R protein. It is known that PEDF-R polypeptide sequence has glycosylation and phosphorylation sites. Although, identification and characterization of PEDF-R isoforms need further evaluation, our finding conclusively verifies a single *Pnpla2* transcript in mouse.

#### Acknowledgements

We thank Grace Woo for preparation of 661W total cell lysate and Dr. Luigi Notari for isolation of total RNA from mouse tissue samples. This work was supported, in part, by National Institutes of Health NEI Intramural Research Program under NEI Project # ZIA EY000306).

#### References

1. Kienesberger PC, Oberer M, Lass A, Zechner R (2009) Mammalian patatin domain containing proteins: a family with diverse lipolytic activities involved in multiple biological functions. J Lipid Res 50 Suppl: S63-68.

- Wilson PA, Gardner SD, Lambie NM, Commans SA, Crowther DJ (2006) Characterization of the human patatin-like phospholipase family. J Lipid Res 47: 1940-1949.
- Zimmermann R, Strauss JG, Haemmerle G, Schoiswohl G, Birner-Gruenberger R, et al. (2004) Fat mobilization in adipose tissue is promoted by adipose triglyceride lipase. Science 306: 1383-1386.
- Notari L, Baladron V, Aroca-Aguilar JD, Balko N, Heredia R, et al. (2006) Identification of a lipase-linked cell membrane receptor for pigment epithelium-derived factor. J Biol Chem 281: 38022-38037.
- Subramanian P, Notario PM, Becerra SP (2010) Pigment epithelium-derived factor receptor (PEDF-R): a plasma membrane-linked phospholipase with PEDF binding affinity. Adv Exp Med Biol 664: 29-37.
- Duncan RE, Wang Y, Ahmadian M, Lu J, Sarkadi-Nagy E, et al. (2010) Characterization of desnutrin functional domains: critical residues for triacylglycerol hydrolysis in cultured cells. J Lipid Res 51: 309-317.
- Lake AC, Sun Y, Li JL, Kim JE, Johnson JW, et al. (2005) Expression, regulation, and triglyceride hydrolase activity of Adiponutrin family members. J Lipid Res 46: 2477-2487.
- Subramanian P, Locatelli-Hoops S, Kenealey J, Desjardin J, Notari L, et al. (2013) Pigment Epithelium-derived Factor (PEDF) Prevents Retinal Cell Death via PEDF Receptor (PEDF-R): IDENTIFICATION OF A FUNCTIONAL LIGAND BINDING SITE. J Biol Chem 288: 23928-23942.
- Barnstable CJ, Tombran-Tink J (2004) Neuroprotective and antiangiogenic actions of PEDF in the eye: molecular targets and therapeutic potential. Prog Retin Eye Res 23: 561-577.
- Becerra SP (2006) Focus on Molecules: Pigment epithelium-derived factor (PEDF). Exp Eye Res 82: 739-740.
- Bouck N (2002) PEDF: anti-angiogenic guardian of ocular function. Trends Mol Med 8: 330-334.
- Balsinde J, Winstead MV, Dennis EA (2002) Phospholipase A(2) regulation of arachidonic acid mobilization. FEBS Lett 531: 2-6.
- Gonzalez R, Jennings LL, Knuth M, Orth AP, Klock HE, et al. (2010) Screening the mammalian extracellular proteome for regulators of embryonic human stem cell pluripotency. Proc Natl Acad Sci U S A 107: 3552-3557.
- Ladhani O, Sánchez-Martínez C, Orgaz JL, Jiménez B, Volpert OV (2011) Pigment epithelium-derived factor blocks tumor extravasation by suppressing amoeboid morphology and mesenchymal proteolysis. Neoplasia 13: 633-642.
- Hirsch J, Johnson CL, Nelius T, Kennedy R, Riese Wd, et al. (2011) PEDF inhibits IL8 production in prostate cancer cells through PEDF receptor/phospholipase A2 and regulation of NF $\kappa$ B and PPAR $\delta$ . Cytokine 55: 202-210.
- Modrek B, Lee C (2002) A genomic view of alternative splicing. Nat Genet 30: 13-19.
- Kanan Y, Jacobi AK, Sawyer K, Mannel DS, Tink JT, et al. (2008) An in-vivo assay to identify compounds protective against light induced apoptosis. Adv Exp Med Biol 613: 61-67.
- Wang F, Zhao Y, Hao Y, Tan Z (2008) Identification of low-abundance alternatively spliced mRNA variants by exon exclusive reverse transcriptase polymerase chain reaction. Anal Biochem 383: 307-310.
- Flicek P, Ahmed I, Amode MR, Barrell D, Beal K, et al. (2013) Ensembl 2013. Nucleic Acids Res 41: D48-55.
- Kent WJ, Sugnet CW, Furey TS, Roskin KM, Pringle TH, et al. (2002) The human genome browser at UCSC. Genome Res 12: 996-1006.
- Nagaraj SH, Gasser RB, Ranganathan S (2007) A hitchhiker's guide to expressed sequence tag (EST) analysis. Brief Bioinform 8: 6-21.